Energy 74 (2014) 950–955

Contents lists available at ScienceDirect

Energy

journal homepage: www.elsevier.com/locate/energy

Combustion of biodiesel in a large-scale laboratory furnace

Caio Pereira, Gongliang Wang, Mário Costa*

IDMEC, Mechanical Engineering Department, Instituto Superior Técnico, Universidade de Lisboa, Lisboa, Portugal

ARTICLE INFO

Article history:
Received 8 October 2013
Received in revised form
22 July 2014
Accepted 23 July 2014
Available online 15 August 2014

Keywords:
Combustion
Biodiesel
Large-scale furnace
Pollutant emissions

ABSTRACT

Combustion tests in a large-scale laboratory furnace were carried out to assess the feasibility of using biodiesel as a fuel in industrial furnaces. For comparison purposes, petroleum-based diesel was also used as a fuel. Initially, the performance of the commercial air-assisted atomizer used in the combustion tests was scrutinized under non-reacting conditions. Subsequently, flue gas data, including PM (particulate matter), were obtained for various flame conditions to quantify the effects of the atomization quality and excess air on combustion performance. The combustion data was complemented with in-flame temperature measurements for two representative furnace operating conditions. The results reveal that (i) CO emissions from biodiesel and diesel combustion are rather similar and not affected by the atomization quality; (ii) NO_x emissions increase slightly as spray quality improves for both liquid fuels, but NO_x emissions from biodiesel combustion are always lower than those from diesel combustion; (iii) CO emissions decrease rapidly for both liquid fuels as the excess air level increases up to an O_2 concentration in the flue gas of 2%, beyond which they remain unchanged; (iv) NO_x emissions increase with an increase in the excess air level for both liquid fuels; (v) the quality of the atomization has a significant impact on PM emissions, with the diesel combustion yielding significantly higher PM emissions than biodiesel combustion; and (vi) diesel combustion originates PM with elements such as Cr, Na, Ni and Pb, while biodiesel combustion produces PM with elements such as Ca, Mg and Fe.

1. Introduction

Intense research is being carried out on the combustion of biodiesel, one of the main alternative fuels available in the world market. Biodiesel is commonly produced by transesterification, which transforms different kinds of vegetable oils into FAME (fatty acids methyl esters) [1,2], used as a fuel in various industrial applications. Current concerns are centred on the emissions of gaseous pollutants, such as CO, HC and NO_x, and also in PM (particulate matter) emissions, which can present harmful and non reversible effects on human health. Against this background, it is important to continue developing strategies to minimize both gaseous and PM pollutant emissions from combustion systems.

Related studies include those of Tashtoush et al. [3], Ng and Gan [4], José et al. [5], Bazooyar et al. [6] and Ghorbani et al. [7]. Tashtoush et al. [3] investigated the combustion characteristics and emissions of the ethyl ester of used palm oil and petroleum diesel fuel in a water-cooled furnace. The authors concluded that biodiesel may lead to higher combustion efficiencies and lower pollutant emissions than petroleum diesel. Ng and Gan [4] examined the combustion of palm oil methyl ester and its blends with diesel in a water-cooled combustor. The work demonstrated the potential use of palm oil biodiesels in small-scale liquid fuel burners, although further work is required to establish the optimum operating parameters and biofuel content for best NO_x and CO emissions trade-off. José et al. [5] evaluated the use of biodiesel and petroleum-based diesel mixtures in a conventional boiler and concluded that the maximum performance of the mixtures requires an adjustment of the fuel parameters depending on the oxygen content of the biodiesel and boiler operating conditions. Bazooyar et al. [6] investigated the combustion of petroleum diesel and biodiesels of grape seed, corn, sunflower, soybean, olive and rice bran oils in a water-cooled combustor. The authors observed that, under certain combustor operating conditions, all vegetable based methyl ester could emit lower gaseous emissions than petroleum diesel. Ghorbani et al. [7] compared the combustion of various biodiesel blends with petroleum diesel in an experimental boiler and observed that generally the pollutant emissions from the biodiesel blends were lower than those from the petroleum diesel.

In this work, combustion tests in a large-scale laboratory furnace were carried out to assess the feasibility of using biodiesel

* Corresponding author. Mechanical Engineering Department, Instituto Superior Técnico, Av. Rovisco Pais, 1049-001 Lisboa, Portugal. Tel.: +351 218417186.
E-mail address: mcosta@ist.utl.pt (M. Costa).

http://dx.doi.org/10.1016/j.energy.2014.07.077
0360-5442/

Nomenclature

d_o	diameter of the fuel-injection orifice
U_a	atomizing air velocity
μ_f	liquid dynamic viscosity
ρ_a	air density
ρ_f	liquid density
σ	air surface tension
σ_f	liquid surface tension

Abbreviations

AFR	atomizing air/fuel ratio
ERZ	external recirculation zone
FAME	fatty acids methyl esters
IRZ	internal recirculation zone
PM	particulate matter
SEM	scanning electron microscope
SMD	Sauter mean diameter

as a fuel in industrial furnaces. For comparison purposes, petroleum diesel was also used as a fuel. Initially, the performance of the commercial air-assisted atomizer used in the combustion tests was scrutinized under non-reacting conditions. Subsequently, flue gas data, including PM, were obtained for various flame conditions to quantify the effects of the atomization quality and excess air on combustion performance. The combustion data was complemented with in-flame temperature measurements for two representative furnace operating conditions.

2. Materials and methods

Fig. 1 shows a schematic of the Instituto Superior Técnico large-scale laboratory furnace and its auxiliary equipment. The furnace is a vertical cylinder 0.6 m in diameter and 2.4 m in length, down-fired along its axis by a swirl burner. The furnace roof and the initial 1.2 m length of the cylindrical walls are refractory-lined. The outer surfaces of the refractory walls are surrounded by cooling water jackets. The remaining 1.2 m length of the wall surfaces are water-cooled only. Fig. 2 shows a schematic of the furnace roof and burner arrangement. The burner consists of a central gun and a secondary air supply in a conventional double-concentric configuration, terminating in a refractory quarl. The secondary air stream is fitted with guide vanes of constant cord and angle of 45° for inducing swirl. The burner gun comprises a removable air-assisted atomizer and a co-axial supply of primary air. In this study, a commercial air-assisted atomizer (Schlick model 0/2 form 6) was used, as shown in Fig. 2. The liquid fuels (biodiesel and diesel) were supplied to the burner with the aid of a nitrogen-pressurized tank, with the liquid fuel flow rate being measured with a calibrated rotameter.

Prior to the combustion tests in the large-scale laboratory furnace, a large number of water sprays produced by the atomizer were characterized under isothermal conditions in a spray test rig using the Phantom V4.2 high speed camera and the Malvern Particle Size Analyzer.

Local mean temperature measurements were obtained using uncoated 76-μm-diameter fine-wire platinum/platinum: 13% rhodium thermocouples. The hot junction was installed and supported on 350-μm wires of the same material as that of the junction. The 350-μm-diameter wires were located in a twin-bore alumina sheath with an external diameter of 4 mm and placed inside a stainless steel tube. The thermocouple probe was mounted on a computer-controlled traverse mechanism that allowed for movements along a furnace diameter. The analogue outputs of the thermocouple were transmitted via A/D boards to a computer where the signals were processed and the mean values computed.

Flue gas composition data were obtained with the aid of a stainless steel water-cooled probe placed at the exhaust duct of the furnace. The probe had a central 2 mm inner diameter tube through which quenched samples were evacuated. This central tube was surrounded by two concentric tubes for probe cooling. The analytical instrumentation included a magnetic pressure analyzer for O_2 measurements, a non-dispersive infrared gas analyzer for CO_2 and CO measurements, and a chemiluminescent analyzer for

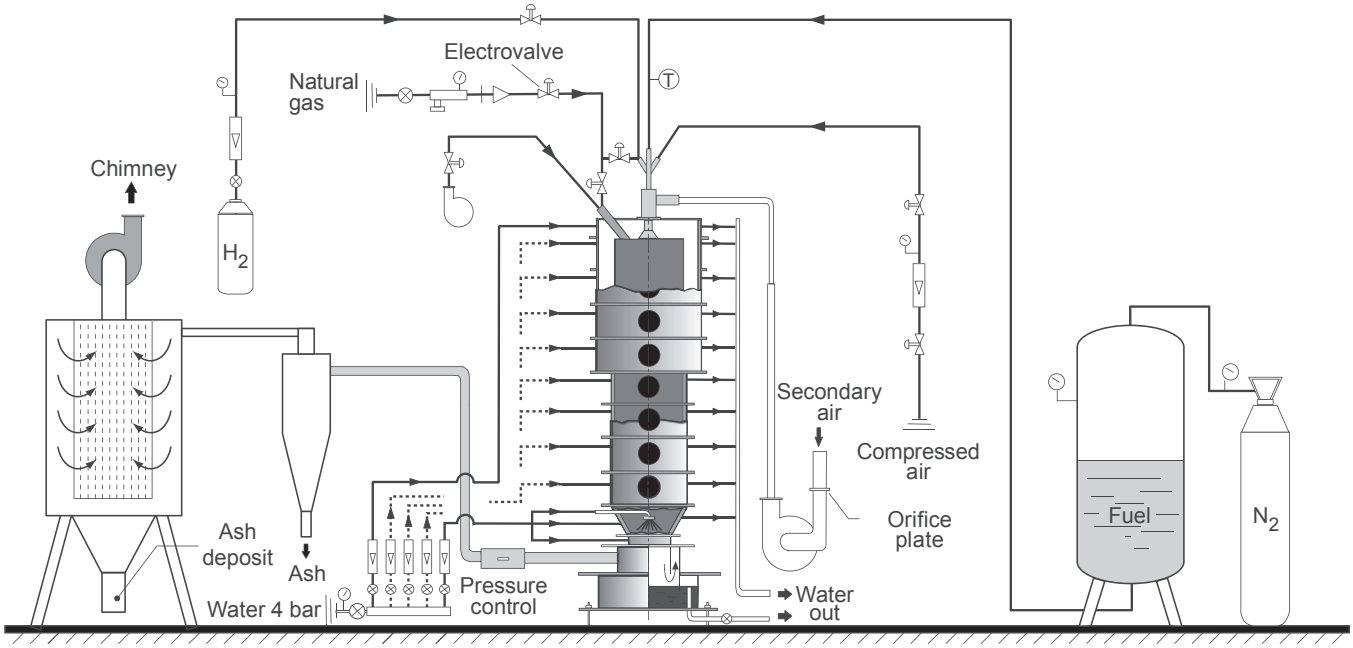

Fig. 1. Schematic of the large-scale furnace and its auxiliary equipment.

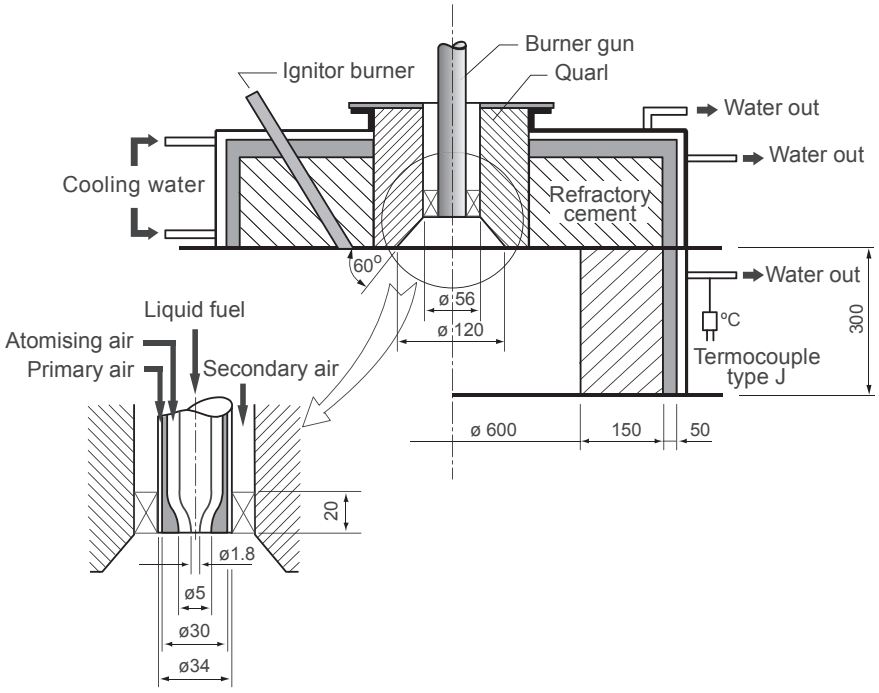

Fig. 2. Schematic of the furnace roof and burner arrangement.

NO_x measurements. Repeatability of these flue gas data was, on average, within 5% of the mean value.

PM sampling was accomplished isokinetically (i.e., sampling at a rate which ensured that the average velocity of the gas entering the probe was the same as that of the gas in the furnace at the sampling point) with the aid of a water-cooled probe placed at the exhaust duct of the furnace. On leaving the probe, the flue gas (10 NL/min) flow through a Tecora total filter holder where the PM were captured in a quartz microfiber placed in the filter holder. To avoid condensation in the filter, the system was maintained at 120 °C with the aid of a resistance. After PM collection, the quartz filter was weighed on a microelectronic balance and the PM concentration calculated. Subsequently, the morphology and chemical composition of the PM samples were examined in a SEM (scanning electron microscope) – JEOL, model JSM-7001F – equipped with an energy dispersive *x*-ray spectroscopy detector. For each sample, the PM chemical composition data were obtained considering five different areas of 50 × 50 μm^2.

Table 1 presents the fatty acids composition of the biodiesel, Table 2 shows the properties of the biodiesel and diesel and Table 3 lists the furnace operating conditions examined in this study. Note that the series number I aims to evaluate the effect of the atomization quality, as typified by the AFR (atomizing air/fuel ratio), on pollutant emissions, while the series number II allows to evaluate the effect of the excess air level on emissions. All emissions were corrected to 6% of oxygen in the combustion products.

Table 1
Fatty acids composition of biodiesel.

Fatty acid	Value (wt%)
Myristic (C 14:0)	1.0
Palmitic (C 16:0)	43.8
Palmitoleic (C 16:1)	0.2
Stearic (C 18:0)	4.4
Oleic (C 18:1)	39.2
Linoleic (C 18:2)	10.4
Linolenic (C 18:3)	0.3
Arachidic (C 20:0)	0.4
Eicosenoic (C 20:1)	0.1
Behenic (C 22:0)	0.1
Lignoceric (C 24:0)	0.1

3. Results and discussion

3.1. Atomization tests

Fig. 3 shows spray images, obtained with the aid of the Phantom V4.2 high speed camera, as function of AFR at a constant water mass flow rate of 12.3 kg/h. The figure reveals the beneficial effect of increasing the AFR on spray quality. The incremental increases in

Table 2
Biodiesel and diesel properties.

Property	Biodiesel	Diesel
Chemical formula	$C_{18.3}H_{34.8}O_2$	$C_{13.3}H_{24.7}O_{<0.01}$
Density @ 15 °C (kg/m^3)	875	836
Viscosity @ 40 °C (mm^2/s)	4.43	2.59
Surface tension @ 40 °C (N/m)	0.028	0.025
Carbon (wt%)	76.68	86.49
Hydrogen (wt%)	12.15	13.48
Oxygen (wt%)	11.17	0.03
Sulphur (mg/kg)	<3	5.9
Nitrogen (mg/kg)	–	28
FAME (vol%)	99.4	0.3
Flash point (°C)	135	58
Low heating value (MJ/kg)	37.79	42.93

Table 3
Furnace operating conditions.

Series number	I	II
Thermal input (kW)	120	120
Fuel inlet temperature (°C)	25	25
AFR	0.5–2.5	2
Flue gas O_2 (dry vol %)	2	1–5

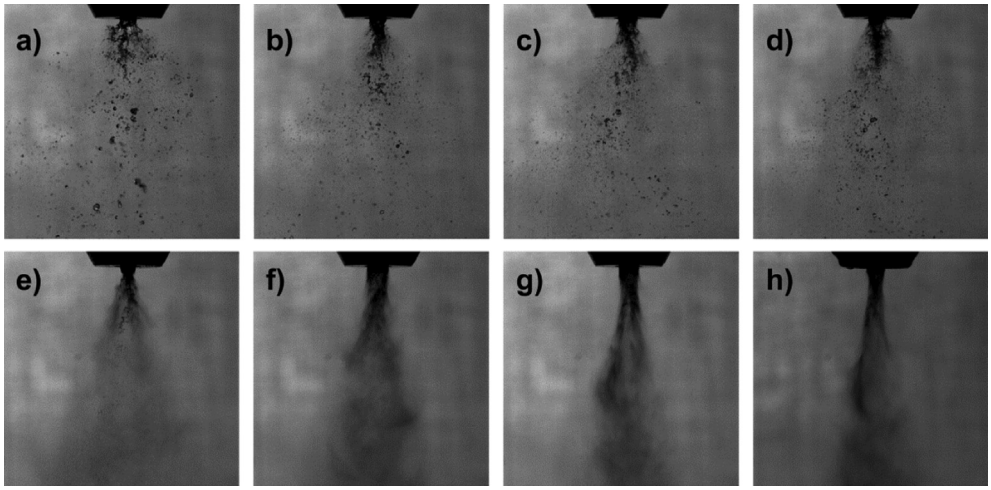

Fig. 3. Spray images as function of AFR at a constant water mass flow rate of 12.3 kg/h. a) AFR = 0.27; b) AFR = 0.36; c) AFR = 0.52; d) AFR = 0.66; e) AFR = 0.85; f) AFR = 1; g) AFR = 1.5; h) AFR = 2.

the air mass flow and, consequently, in the atomizing air velocity, result in an improvement in atomisation as a consequence of there being more kinetic energy available to disintegrate the liquid jet. As the AFR increases the break-up length reduces and there is clear evidence of an improvement in overall spray quality with the ligaments and large droplets being hardly identifiable for AFR > 0.8 owing to their rapid disintegration.

The present spray images allowed determining the spray cone angle, which is an important spray characteristic. Fig. 4 shows the spray cone angle as a function of the AFR for three water mass flow rates. It is seen that the spray cone angle decreases as AFR increases regardless of the liquid mass flow rate. In particular, for a water mass flow rate of 12.3 kg/h the spray cone angle decreases from around 65° down to 15°. In order to assess the evolution of the spray cone angle with the AFR for diesel and biodiesel sprays we performed a limited number of tests for these liquid fuels and concluded that the differences in relation to the corresponding water spray cone angles were marginal.

Fig. 5 shows the SMD (Sauter mean diameter) as a function of AFR for two water mass flow rates. The measurements were obtained with the aid of the Malvern Particle Size Analyzer by placing the laser beam across the spray at a distance of 40 mm from the atomizer tip. The figure reveals that the spray quality, as typified by the SMD, increases significantly as AFR increases up to around 0.5, beyond which the improvements in spray quality are marginal, regardless of the water mass flow rate. At low values of AFR, the kinetic energy of the atomizing air is insufficient to overcome the viscous and surface tension forces, which oppose the disintegration of the liquid. As the AFR increases, both the atomizing air mass flow rate and its kinetic energy increase and, consequently, more energy is available to shatter the fuel jet into droplets. The levelling off of the curves beyond a certain value of AFR suggests that above this value the additional atomizing air does not effectively interact with the fuel jet. A similar behaviour is expected for the biodiesel and diesel jets since the performance of the atomizer is dominated by the AFR.

Based on the measured data for the water sprays, a correlation was derived to predict SMD for the present atomizer as follows:

$$\frac{\mathrm{SMD}}{d_o} = 0.3\left(\frac{\sigma}{\rho_a U_a^2 d_o}\right)^{0.67}\left(1+\frac{1}{\mathrm{AFR}}\right)^{0.67} + 1.55\left(\frac{\mu_f^2}{\sigma_f \rho_f d_0}\right)^{0.6}\left(1+\frac{1}{\mathrm{AFR}}\right)^{0.3} \quad (1)$$

where d_o is the diameter of the fuel-injection orifice, σ is air surface tension, ρ_a is the air density, U_a is the atomizing air velocity, μ_f is the liquid dynamic viscosity, σ_f is the liquid surface tension and ρ_f is the liquid density. This equation was used to calculate the SMD for both fuels (biodiesel and diesel) considered in the following section.

3.2. Combustion tests

Before examining the combustion data, a qualitative description of the structure of the near burner region, based on our previous studies in the present furnace [e.g., Refs. [8–10]], will be of use in understanding the discussion that follows. The secondary air swirl number used in the present study is large enough to generate a

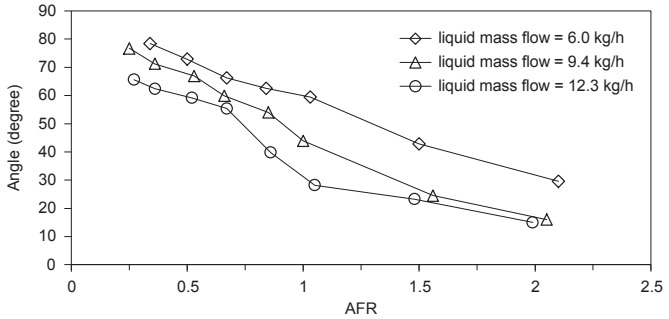

Fig. 4. Spray cone angle as a function of AFR for three water mass flow rates.

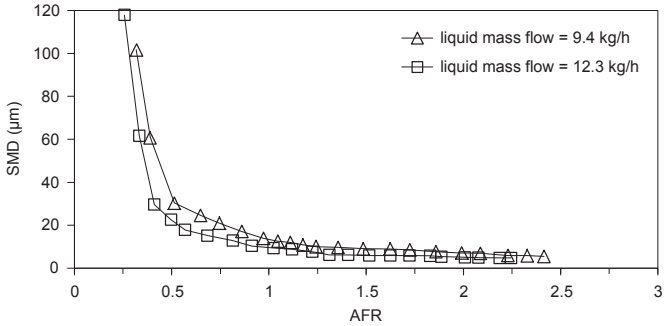

Fig. 5. SMD as a function of AFR for two water mass flow rates.

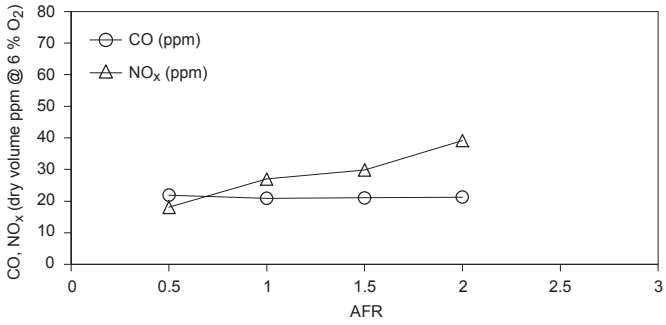

Fig. 6. Effect of AFR on CO and NO_x emissions for biodiesel.

strong IRZ (internal recirculation zone). An ERZ (external recirculation zone) is also established due to flow separation at the quarl exit. The IRZ plays the crucial role in the stabilization process of the present flames. This is a result of the primary jet, containing the liquid fuel droplets, being directly introduced into the IRZ wherein it penetrates to an extent dependent upon its momentum. The fast mixing of the droplets with the hot recirculated gases in the IRZ results in a sharp temperature increase and their consequent high vaporization rates.

Figs. 6 and 7 show the effect of the AFR on the CO and NO_x emissions for biodiesel and diesel, respectively. It is seen that the CO emissions resulting from biodiesel and diesel combustion are rather similar and not affected by the atomization quality, as typified by the AFR. Despite Eq. (1) yielding values for SMD slightly higher for biodiesel than for diesel, the IRZ is strong enough to handle successfully the combustion of the poor quality sprays as indicated by the relatively low CO emissions (around 20 ppm for all cases). Figs. 6 and 7 also show that the NO_x emissions increase slightly as AFR increases for both liquid fuels because the effect of increasing the AFR from 0.5 to 2 is to increase the combustion intensity in the near burner region and, consequently, the gas temperatures. This means a gradual increase in the thermal NO formation as AFR increases. In addition, Figs. 6 and 7 reveal that NO_x emissions from biodiesel combustion are always lower than those from diesel combustion. Two reasons support this evidence. First, the fuel bound nitrogen present in the diesel, as shown in Table 2, may lead to the formation of NO via the fuel mechanism and, second, the biodiesel firing leads to lower temperatures in the near burner region, as shown in Fig. 8, which reduces the formation of NO via the thermal mechanism. These results are consistent with those obtained by Tashtoush et al. [3], who also reported higher NO_x emissions for petroleum diesel than for biodiesel due to its higher nitrogen content.

Figs. 9 and 10 show the effect of the excess air level on the CO and NO_x emissions for biodiesel and diesel, respectively. Again, the values of the CO emissions are similar for both liquid fuels, decreasing rapidly until an O_2 concentration in the flue gas of 2%, beyond which they remain unchanged. The relatively high CO emissions observed at low excess air levels is a direct consequence of the lower O_2 availability, which presumably originates fuel-rich zones in the central region of the spray, leading to incomplete combustion and, therefore, higher emissions of CO. As the excess air increases, more O_2 becomes available and, thus, the CO emissions decrease significantly. Figs. 9 and 10 also reveal that the NO_x emissions, lower for biodiesel combustion, increase with an

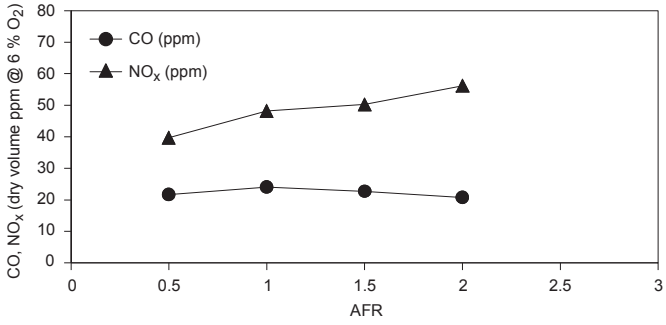

Fig. 7. Effect of AFR on CO and NO_x emissions for diesel.

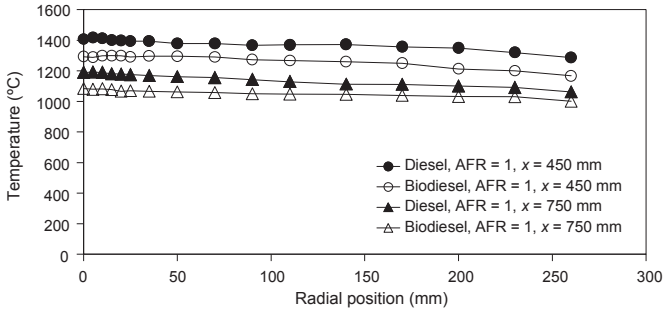

Fig. 8. In-flame temperature radial profiles for biodiesel and diesel firing. (x represents the axial distance from furnace roof).

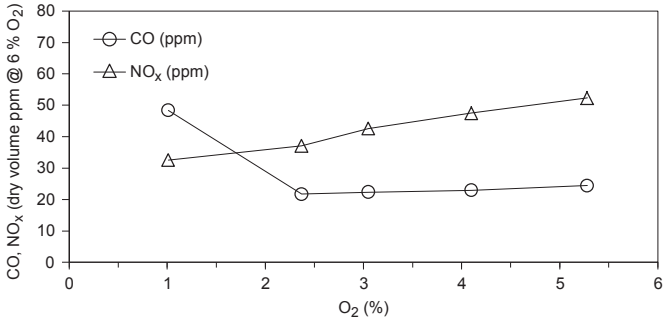

Fig. 9. Effect of excess air level on CO and NO_x emissions for biodiesel.

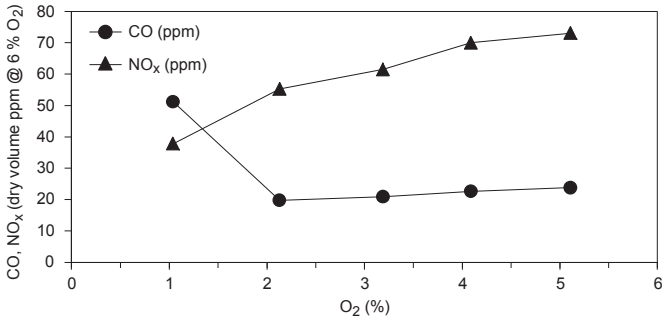

Fig. 10. Effect of excess air level on CO and NO_x emissions for diesel.

Table 4
PM emissions.

Test conditions			PM emissions (mg/Nm^3@6% O_2)
Fuel	AFR	Flue gas O_2 (dry vol %)	
Biodiesel	0.5	2	98.2
Biodiesel	2	2	23.0
Diesel	2	2	90.2

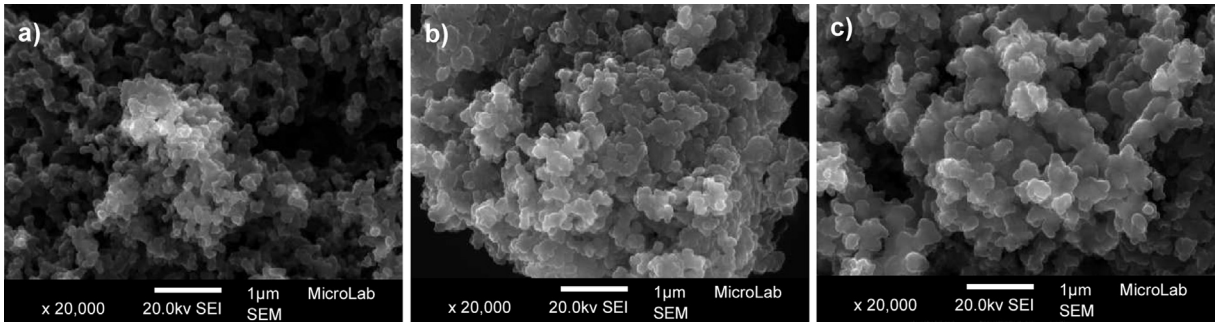

Fig. 11. Typical SEM images of PM. a) Biodiesel, AFR = 0.5, flue gas O_2 = 2%; b) biodiesel, AFR = 2, flue gas O_2 = 2%; c) diesel, AFR = 2, Flue gas O_2 = 2%.

increase in the excess air level for both liquid fuels. Increasing the excess of air enhances mixing and combustion intensity, resulting in higher flame temperatures, which promotes NO formation via the thermal mechanism. It is interesting to observe that the increase in NO_x emissions with the excess air level is more accentuated in diesel combustion than in biodiesel combustion.

Table 4 shows PM emissions for three furnace operating conditions. It is seen that the quality of the atomization has a significant impact on PM emissions and that diesel combustion yields significantly higher concentration of PM than biodiesel combustion.

Fig. 11 shows typical SEM images of the PM for the three furnace operating conditions listed in Table 4. It is clear that PM are composed mainly by soot (~90 wt% of carbon) aggregates. Apart from C and O, the chemical analysis also revealed the presence of minor elements such as Cr, Na, Ni and Pb in the PM from the diesel combustion and elements such as Ca, Mg and Fe in the PM from the biodiesel combustion.

4. Conclusions

The main conclusions of this study are as follows:

- CO emissions from biodiesel and diesel combustion are rather similar and not affected by the atomization quality.
- NO_x emissions increase slightly as spray quality improves for both liquid fuels, but NO_x emissions from biodiesel combustion are always lower than those from diesel combustion.
- CO emissions decrease rapidly for both liquid fuels as the excess air level increases up to an O_2 concentration in the flue gas of 2%, beyond which they remain unchanged.
- NO_x emissions increase with an increase in the excess air level for both liquid fuels.
- The quality of the atomization has a significant impact on PM emissions, with the diesel combustion yielding significantly higher PM emissions than the biodiesel combustion.
- Diesel combustion originates PM with elements such as Cr, Na, Ni and Pb, while biodiesel combustion produces PM with elements such as Ca, Mg and Fe.

Acknowledgements

Financial support for this work was provided by the European Commission under the project “New Method for Superior Integrated Hydrogen Generation System 2+”, contract number 278138, and is acknowledged with gratitude. Gongliang Wang is pleased to acknowledge the China Scholarship Council for the provision of a scholarship (CSC no. 2008609127).

References

[1] Hájek M, Skopal F, Capek L, Cernoch M, Kutálek P. Ethanolysis of rapeseed oil by KOH as homogeneous and as heterogeneous catalyst supported on alumina and CaO. Energy 2012;48:392–7.
[2] Lee HV, Taufiq-Yap YH, Hussein MZ, Yunus R. Transesterification of jatropha oil with methanol over MgeZn mixed metal oxide catalysts. Energy 2013;49:12–8.
[3] Tashtoush G, Al-Widyan MI, Al-Shyoukh AO. Combustion performance and emissions of ethyl ester of a waste vegetable oil in a water-cooled furnace. Appl Therm Eng 2003;23:285–93.
[4] Ng HK, Gan S. Combustion performance and exhaust emissions from the non-pressurised combustion of palm oil biodiesel blends. Appl Therm Eng 2010;30:2476–84.
[5] José JS, Al-Kassir A, López Sastre JA, Gañán J. Analysis of biodiesel combustion in a boiler with a pressure operated mechanical pulverisation burner. Fuel Process Technol 2011;92:271–7.
[6] Bazooyar B, Ghorbani A, Shariati A. Combustion performance and emissions of petrodiesel and biodiesels based on various vegetable oils in a semi industrial boiler. Fuel 2011;90:3078–92.
[7] Ghorbani A, Bazooyar B, Shariati A, Jokar SM, Ajami H, Naderi A. A comparative study of combustion performance and emission of biodiesel blends and diesel in an experimental boiler. Appl Energy 2011;88:4725–32.
[8] Rebola A, Costa M. Simultaneous reduction of NO_x and particulate emissions from heavy fuel oil-fired furnaces. Proc Combust Inst 2002;29:2243–50.
[9] Casaca C, Costa M. Co-combustion of biomass in a natural gas fired furnace. Combust Sci Technol 2003;175:1953–77.
[10] Saario A, Rebola A, Coelho PJ, Costa M, Oksanen A. Heavy fuel oil combustion in a cylindrical laboratory furnace: measurements and modelling. Fuel 2005;84:359–69.